Thermal behavior of curved roof buildings exposed to solar radiation and wind flow for various orientations

Article *in* Applied Energy · August 2008
DOI: 10.1016/j.apenergy.2008.01.002

2 authors:

Mahshid Hadavand
University of New Brunswick
11 PUBLICATIONS **51** CITATIONS
SEE PROFILE

M. Yaghoubi
Shiraz University
165 PUBLICATIONS **1,657** CITATIONS
SEE PROFILE

Available online at www.sciencedirect.com
ScienceDirect
Applied Energy 85 (2008) 663–679
APPLIED ENERGY
www.elsevier.com/locate/apenergy

Thermal behavior of curved roof buildings exposed to solar radiation and wind flow for various orientations

M. Hadavand [a,1], M. Yaghoubi [a,b,*]

[a] *Engineering School, Shiraz University, Shiraz 71348-51154, Iran*
[b] *Academy of Sciences, Islamic Republic of Iran*

Received 15 September 2007; received in revised form 9 January 2008; accepted 14 January 2008
Available online 6 March 2008

Abstract

In this study air flow, solar radiation and heat transfer from a two dimensional curved roof with north-south and east-west faced are determined and results are compared with flat roof for the same size and orientation. Comparison are performed for their corresponding roof surface temperature, and heat flow for several roof rim angles and also for various wind flow velocities, as well as for different wind directions. Turbulence is modeled by RNG k–ε method and solar radiation distribution over the roof is determined based on an appropriate model applicable to hot arid regions of Iran. Solar radiation is calculated based on the summation of beam and diffuse radiation and ground reflected radiation. For certain inside roof temperature, over all heat transfer to the building is determined with day time for various wind flows and arc shapes and results are compared with flat roof. It was found that various wind flow condition over the vaulted roof makes substantial difference on the convection heat transfer coefficient and finally on the rate of heat transfer to the building with respect to flat roof. Based on heat transfer simulation, roof temperature, heat transfer convection coefficient and heat flow though the vault for different roof arrangement and flat roofs have been determined and advantages of specific vault orientation and wind direction are specified.

Keywords: Arc roof; Heat exchange; Cooling load; Computational heat transfer

1. Introduction

Curved roofs buildings have been the most important element of architecture in the middle-east area and especially in Iran during the past centuries. Such buildings have been especially built for large state or religious spaces mainly cathedrals, churches and mosques all over the world and also for buildings such as single-family dwellings, Arab houses and Inuit Igloos. In hot arid region of Iran, most of bazaars, water cisterns and many old houses have roof in the form of semi sphere or various vaulted structures [1]. Domed and vaulted roofs in

* Corresponding author. Address: Engineering School, Shiraz University, Shiraz 71348-51154, Iran. Tel.: +98 711 6274841.
E-mail address: yaghoub@shirazu.ac.ir (M. Yaghoubi).
[1] Address: Department of Mechanical Engineering, University of New Brunswick, P.O. Box 4400, Fredericton, NB, Canada E3B 5A3.

0306-2619/$ - see front matter © 2008 Elsevier Ltd. All rights reserved.
doi:10.1016/j.apenergy.2008.01.002

Nomenclature

A_1, A_2, A_3	constant parameter in Daneshyar model
C_μ, $C_{1\varepsilon}$, $C_{2\varepsilon}$	constant coefficient in turbulence model
C_P	pressure coefficient
C_p	specific heat (j/kg K)
CF	cloud factor
F_{wg}	shape factor from roof surface to ground
F_{ws}	shape factor from roof to sky
G_{beam}	solar beam radiation (W/m^2)
G_{diff}	diffuse radiation (W/m^2)
G_t	total energy which receive on a horizontal surface (W/m^2)
h	convective heat transfer coefficient (W/m^2K)
H	height of building (m)
k	turbulent kinetic energy (m^2/s^2)
$\overline{Nu}$	mean Nusselt number $\overline{Nu} = \bar{h}H/\lambda$
P	pressure (Pa)
Pr	Prandtl number
Pr_t	turbulent Prandtl number
Q	heat flux (W/m^2)
Re	Reynolds number $Re = \rho U_\infty H/\mu$
S_{ij}	mean strain rate transform (s^{-1})
T	temperature (K)
t	time (s)
u_i	index notation of velocity components (m/s)
U_∞	free wind velocity (m/s)
x_i	stream wise and cross-stream coordinates (m)
x^*	x/H
α_k, α_ε	constant coefficient in turbulence model
α	absorptance coefficient
α_s	solar altitude angle
β_o	slop angle
δ_{ij}	Kronecker delta
ε	turbulent dissipation rate (m^2/s^3)
ε	emittance
η, η_o	parameters in RNG k–ε model
θ_0	vaulted roof rim angle
κ	Von Karman's constant
λ	thermal conductivity (W/mK)
μ, μ_t	laminar and turbulent viscosity (kg/ms)
ρ	density (kg/m^3)
ρ_g	ground reflectance
σ	Stefan-Boltzmann constant (W/m^2K^4)

Subscripts

a	ambient air
cond	conduction
conv	convection
in	internal roof surface
r	roof

s	solar
sky	sky

Iran are mostly built with adobe or mud bricks. Great usage of these materials in building construction is due to the abundant of such material and lack of other materials such as stone, timber, etc. However, their low costs and good thermal performance must have been the main reasons for their popularity [2]. Mainstone [3] believed that buildings with curved roofs in hot dry climate maintained lower temperatures during the hot summer months and reflect more radiation than flat roofs. Based on the fact that the surface area of vault or dome is larger than that of flat surface covering an equivalent base area, Fathy [4] suggested that the intensity of solar radiation is spread over a larger area and the average heat increase of the roof and heat transmission to the interior are reduced.

Thermal study of wind flow from vaulted roof buildings are not considerable. There are some qualitative studies as well as typical flow visualizations for single vaulted roofs. Yaghoubi [5] has carried some experiments on simple models of vaulted roofs buildings in a two dimensional low speed wind tunnel for low velocity smoke flows. Later Sabzevari and Yaghoubi [6] tested some flow visualization on a composition of models of isolated cuboid, cuboid with domed roof and multiple domed roof buildings subjected to a light boundary layer wind in a wind tunnel and identified various flow patterns. These studies emphasized on higher wind velocity and pressure difference above vaulted roof with respect to flat roofs. Hadavand et al. [7] studied fluid flow over vaulted roofs numerically and compared them with flat roof for only north-south building orientation.

Pearlmutter [8] has made the first attempt to quantitatively compare thermal behavior of vaulted and flat roofs in terms of indoor temperatures. It was shown that the vaulted roof has greater thermal stability and potentially favorable daytime temperature. Gadi [9] studied a new design of roof system to induce natural ventilation and cooling in summer and to provide heating in winter by combining a transparent dome with a pitch thermal roof. Tang et al. [10] compared the amount of solar heat to domed roofs and flat roofs. They reported that the ratio of radiation absorbed by a curved roof to that absorbed by a flat one increases with increase of rim angle, but it is insignificantly affected by climate characteristics and site latitude. They have made another attempt to calculate heat flux and daily heat flow through curved roofs into an air-conditioned building based on three dimensional unsteady heat transfer equations including solar radiation [11]. They have found that the amount of heat transfer to a cylindrical building with north-south and east-west faced roofs are 20% and 27% more than flat roofs respectively for rim angle of 180°. This is mainly attributed to the assumption of equal convective heat transfer between the enlarged curved roof and ambient air.

Tang et al. [12] in their recent studies have shown that a non-air-conditioned building with a vaulted roof, irrespective of building's type, has lower indoor air temperature as compared to those with a flat roof during the day time under a typical hot dry climate condition.

Hadavand et al. [13] most recently have made the first attempt to explore east-west direction of wind flow around north-south vaulted roofs and flat roof buildings. Thermal analysis of such roofs are carried by considering effects of combined convection and solar radiation. They have found that for rim angles of vault more than about 130° heat flow is more than flat roof. Hadavand et al. [14] in another study compared flow field around different building geometries of flat and vaulted roofs and also determined corresponding heat flow and Nusselt number for these roofs. They reported that for larger width of vaulted roof, Nusselt number on the back side of vault improves because separation point moved further closer to the leeward wall of the building.

The aim of the present study is to compare transient heat transfer from vaulted roofs and flat roofs for the same solar and environmental condition and to determine the effect of wind direction and building orientation on the buildings heat gain and roof surface transient temperature distribution. For this analysis, wind has been assumed to blow from east and also from west directions to a north-south building. Computation is also carried out when the building is oriented east-west direction and wind blows from south or from north while solar radiation has its east-west rotation.

2. Mathematical method

In order to compare heat transfer from flat and vaulted roof buildings, domain of study contains steady fluid domain for wind flow and transient convection heat transfer, and solid roof layer for transient heat conduction. Solar radiation over the roof surface increases the heat load during the day, but wind on the other side has an effective role to increase the rate of heat transfer and reduction of heat load to the building. Schematic of a sample vaulted roof building for various cases are illustrated in Fig. 1. In this configuration, H is constant but U_∞ and roof rim angle 'θ_0' varied to consider all possible configurations.

For the analysis of wind flow around buildings the flow velocity and its direction during the day is assumed constant. Heat transfer to the buildings varies during 24 h of a day, because ambient temperature changes and solar radiation varies with time as sun moves from east to west. Therefore heat transfer to the roof which includes: convection, solar radiation, heat transfer exchange with sky and conduction through the roof has unsteady condition.

Wind is naturally turbulent so a turbulence model should be used for studying wind flow around buildings. In the present analysis RNG k–ε turbulence model [15] is used to simulate the flow field around the building models. This turbulence scheme is more responsible to the effects of rapid strain and streamlines curvature, flow separation, reattachment and recirculation zones than standard k–ε model and widely used for wind flow studies [13,14].

2.1. Basic flow equations

By applying time-averaging procedures to conservation equations, the basic equations that govern the mean flow quantities for incompressible turbulent flow can be described as follows.

$$\text{Mass continuity equation}: \frac{\partial \bar{u}_i}{\partial x_i} = 0 \tag{1}$$

$$\text{Momentum equation}: \frac{\partial}{\partial x_j}(\rho \bar{u}_i \bar{u}_j - \bar{\tau}_{ij}) = -\frac{\partial \overline{P}}{\partial x_i} \tag{2}$$

$$\text{Stress equation}: \bar{\tau}_{ij} = 2\mu S_{ij} - \frac{2}{3}\mu_t \frac{\partial \bar{u}_k}{\partial x_k}\delta_{ij} \tag{3}$$

$$\text{Turbulent viscosity}: \mu_t = \frac{\rho C \mu k^2}{\varepsilon} \tag{4}$$

The variables designated by the superscript "-" are time averaged values. The distortion rate tensor S_{ij} and the Kronecker delta function δ_{ij} can be written as

$$S_{ij} = \frac{1}{2}\left(\frac{\partial \bar{u}_i}{\partial x_j} + \frac{\partial \bar{u}_j}{\partial x_i}\right) \tag{5}$$

$$\delta_{ij} = \begin{cases} 1 & i = j \\ 0 & i \neq j \end{cases} \tag{6}$$

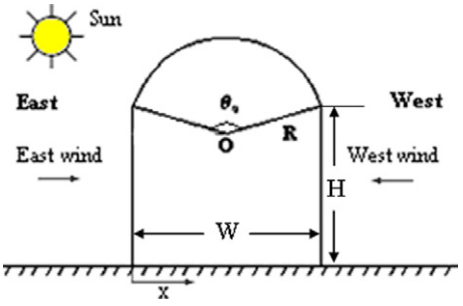

Fig. 1. A north-south vaulted roof building exposed to wind flow from east or from west (W = H).

2.2. RNG k–ε turbulent model

Yakhot and Orszag [15] proposed a variant of the k–ε model such that its performance characteristics were improved relative to the standard model as follows:

$$\text{Turbulent kinetic energy equation is : } \frac{\partial \rho \bar{u}_i k}{\partial x_i} = \frac{\partial}{\partial x_i}\left(\alpha_k \mu_{\text{eff}} \frac{\partial k}{\partial x_i}\right) + \mu_t S^2 - \rho\varepsilon \tag{7}$$

$$\text{Turbulent energy dissipation rate equation is : } \frac{\partial \rho \bar{u}_i \varepsilon}{\partial x_i} = \frac{\partial}{\partial x_i}\left(\alpha_\varepsilon \mu_{\text{eff}} \frac{\partial \varepsilon}{\partial x_i}\right) + C_{1\varepsilon}\mu_t S^2 \frac{\varepsilon}{k} - C^*_{2\varepsilon}\rho\frac{\varepsilon^2}{k} \tag{8}$$

where the effective viscosity, μ_{eff} and the mean rate of strain tensor, S are defined as $\mu_{\text{eff}} = \mu + \mu_t$ and $S = \sqrt{2S_{ij}S_{ij}}$, respectively. $C^*_{2\varepsilon}$ contains the additional source, which is the main difference between the RNG k–ε turbulence models and the standard k–ε turbulence models. It is constant for standard k–ε model but for RNG, $C^*_{2\varepsilon}$ takes the following form:

$$C^*_{2\varepsilon} = C_{2\varepsilon} + \frac{C_\mu \eta^3 (1 - \eta/\eta_0)}{1 + \beta\eta^3} \tag{9}$$

where $\eta = Sk/\varepsilon$, $\eta_0 = 4.38$, $\beta = 0.012$ [15]. The other experimental constants in the above equations are:

$$\alpha_k = \alpha_\varepsilon = 1.393; \quad C_{1\varepsilon} = 1.42; \quad C_{2\varepsilon} = 1.68; \quad C_\mu = 0.0845$$

2.3. Energy equation

Transient energy equation is used for calculation of convection heat transfer from the roof. Energy equation for this part is:

$$\frac{\partial \overline{T}}{\partial t} + \frac{\partial u_i \overline{T}}{\partial x_i} = \frac{\partial}{\partial x_i}\left[\left(\frac{k_a}{\rho_a C_{p_a}} + \frac{\mu_t}{Pr_t}\right)\frac{\partial \overline{T}}{\partial x_i}\right] \quad (i = 1, 2) \tag{10}$$

2.4. Conduction heat transfer equation

Transient conduction heat transfer through the roof layer is determined from the Fourier's equation.

$$\rho_r C_{p_r} \frac{\partial T_r}{\partial t} = \frac{\partial}{\partial x_i}\left(\lambda_r \frac{\partial T_r}{\partial x_i}\right) \quad (i = 1, 2) \tag{11}$$

2.5. Solar radiation

A predominant characteristic of hot-arid zones is the high intensity of solar radiation on summer days. Solar absorptance of a surface depends on the incidence angle of solar rays and properties of the surface [16]. Total instantaneous solar radiation over a surface is the summation of direct beam radiation $G_b(t)$ and diffuse $G_d(t)$.

$$G_t(t) = (G_b(t) + G_d(t))\alpha \tag{12}$$

Diffuse radiation is included of solar sky diffuse radiation and also radiation reflected from ground $G_d = G_{\text{diffuse}} + G_{\text{ground}}$.

In the present study the model of Daneshyar [17] is employed to evaluate beam and diffuse radiation. In this model, the effects of clouds and air mass on the estimation of solar irradiation for Iranian cities are considered. According to Daneshyar [17] solar beam and diffuse radiation are as follows:

$$G_{\text{beam}} = (1 - \text{CF})G_c[1 - \exp(-4.2972\alpha_s)]\cos\theta_i, \quad G_c = 950.61\ (\text{W/m}^2), \quad \alpha_s : \text{radian} \tag{13}$$

θ_i is incidence angle and CF is cloud factor. CF is a parameter which indicates amount of cloud, dust and air mass in the sky. CF = 0 indicates a clear sky and CF = 1 indicates the sky is fully covered with clouds. Daneshyar [17] is determined this parameter for various cities of Iran for every month based on 10 years of statistical data for Iran cities. Solar sky diffuse radiation is obtained based on the following correlation [17].

$$G_{\text{diffuse}} = (A_1 + A_2(\alpha_s) + A_3(\text{CF}))F_{ws}$$
$$A_1 = 1.5352, \quad A_2 = 120.6093, \quad A_3 = 121.301 \tag{14}$$

where F_{ws} is shape factor of radiation exchange from roof to sky which is $F_{ws} = \frac{1+\cos\beta_o}{2}$, and β_o is surface tilt angle.

The amount of heat flux reflected from ground based on the following formulation.

$$G_{\text{ground}} = G_t.\rho_g \cdot F_{wg} \tag{15}$$

G_t is the total amount of solar radiation on the ground surface, and F_{wg} the shape factor of radiation exchange from roof surface to ground which is $F_{wg} = \frac{1-\cos\beta_o}{2}$. Reflectance of ground is considered as $\rho_g = 0.2$. It is clear from formulation that ground reflected radiation must be taken into account for vaulted roofs, but flat roofs do not receive ground reflected radiation. In order to estimate incident solar radiation on a vault roof, the vault surface is fitted by means of several small flat rectangles with the width of grid size on the roof and solar radiation is computed for these elements at different times of the day corresponding to its solar incident angle.

2.6. Heat transfer with sky

Heat transfer with sky in desert communities has effective role on the rate of heat transfer. It is calculated from the following formulation:

$$q''_{\text{sky}} = \sigma\varepsilon(T^4_{\text{sur}} - T^4_{\text{sky}})\left(\frac{1+\cos\beta_o}{2}\right), \quad \sigma = 5.67\times10^{-8}\ (\text{W/m}^2\ \text{K}^4),\ \varepsilon = 0.8 \tag{16}$$

T_{sky} is the equivalent sky temperature in degree of Kelvin which can be determined by $T_{\text{sky}} = 0.0552T^{1.5}_{\text{amb}}$.

Governing equations are non-dimensionalized and transferred to the curve-linear coordinate [18] and solved numerically for special boundary and initial conditions for various vaulted roofs as shown in Fig. 2.

3. Boundary conditions

Solution of the elliptic equations requires that the boundary conditions be specified along the entire boundaries that enclose the flow filed. Wind profile of $u_{in} = 1.104U_\infty y^{1/7}$ is imposed for inlet, x-direction velocity and for y-direction velocity, $v_{in} = 0$ is imposed similar to the previous studies of authors [13,14]. Across the outlet far from the building, zero gradients of variables in the stream wise direction are considered, $\partial(\,)/\partial x = 0$. For upper boundary zero gradients of variables in y-direction $\partial(\,)/\partial y = 0$ are assumed. Turbulent kinetic energy and its dissipation rate for the first grid point near the walls are determined by the standard log-low based wall function [19]. For all points near the walls $y^+ (y^+ = yu_\tau/v$ where u_τ is the friction velocity) is taken more than 30 to be located in turbulent region. Boundary condition for turbulent kinetic energy imposed at the wall is $\partial k/\partial n = 0$ where n is the local coordinate normal to the wall. Turbulence dissipation rate, ε, for the first grid point near the walls is calculated by $\varepsilon_p = \frac{C_\mu^{3/4}k_p^{3/2}}{\kappa y_p}$, where y_p is the length of the first grid from the solid walls and k_p is the turbulent kinetic energy in wall-adjacent cell.

Ambient air temperature changes during the day and obtained from the following relation [13]:

$$T_a = \left(\frac{T_{\max}+T_{\min}}{2}\right) + \left(\frac{T_{\max}-T_{\min}}{2}\right)\cos\left(\frac{\pi(t-15)}{12}\right) \tag{17}$$

where $T_{\max}$, $T_{\min}$ are maximum and minimum ambient air temperature during the day. Inside surface roof temperature is imposed constant of $T_{in} = 27$ °C. Heat transfer for external surface of the roof could be expressed by:

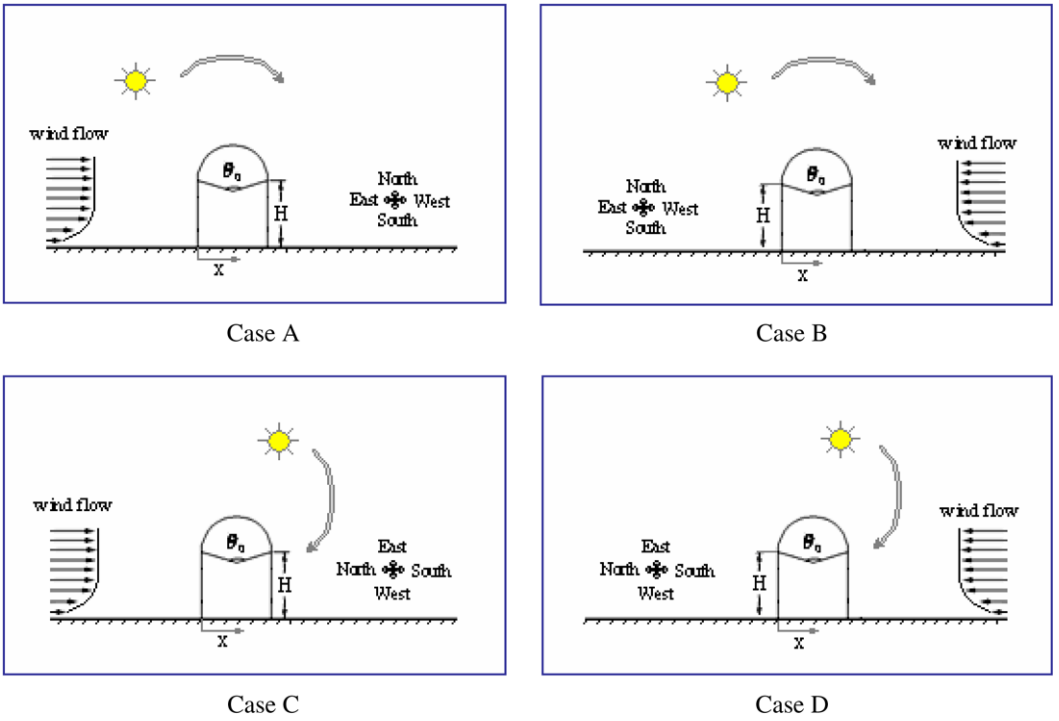

Fig. 2. Various arrangement of building and wind directions.

$$(q_s + q_{cond} + q_{conv} + q_{sky})A_c = \rho_r C_{p_r} \Delta V \frac{\partial T}{\partial t} \tag{18}$$

where q_s is the amount of solar radiation which is absorbed by roof surface, q_{cond} the conduction heat transfer to the lower grid of the roof, q_{conv} the convection heat transfer with ambient air and q_{sky} the amount of heat transfer exchange with sky. ΔV is the volume and A_c is the exposed surface area in each control volume. Insulated conditions are considered for ground surfaces and vertical walls of the buildings.

4. Methodology of numerical calculation

Heat transfer equations dealing with heat transfer through curved and flat roofs are almost impossible to be solved by analytical methods due to the variation of solar radiation and ambient temperature. Therefore, finite volume method is be used to discretize the governing partial differential Eqs. (1), (2), (7), (8), (10) and (11) into a series of algebraic equations. The algebraic equations are solved by using 3DM algorithm.

4.1. Numerical modeling

To study flow field and heat transfer for vaulted and flat roofs thoroughly, the computational domain contains two parts, flow domain and solid domain. In the flow domain, an entrance region far from the building models for applying free stream condition is adopted. The outlet boundaries should be far enough that the results be independent from the outlet boundary position.

Table 1 shows typical results of domain study for 180° rim angle curved roof at $Re = 2 \times 10^6$. Grids for vaulted roof are generated from the best combination of algebraic and differential methods in the flow domain. The numerical solution should be independent of grid size and for this respect, several grid distributions were studied. For each grid size, averaged Nusselt number on the roof is determined and typical calculation is presented in Table 2. From these results and also comparing the values of pressure and velocity values for each grid, it is found that for a typical vault roof with 180° rim angle, the number of grid points in x-, y-direction of

Table 1
The effect of domain size on the averaged Nusselt number ($\theta_0 = 180°$ and $Re = 2 \times 10^6$)

Domain size	$\overline{Nu}$
10H × 22H	5328.5
12H × 25H	5279.3

Table 2
Grid independent study for $\theta_0 = 180°$ and $Re = 2 \times 10^6$

Grids	$\overline{Nu}$
120 × 75	4765.2
150 × 90	5162.7
170 × 100	5328.5
200 × 115	5376.4

170 × 100 is adequate. The grids are non-uniform, with reduced size adjacent to the building roof and walls where the velocity gradient are large and recirculation is expected to develop in these regions. The grid spacing is large far from the building where the flow is without any considerable variation. Typical grid configuration for a vaulted roof building of $\theta_0 = 90°$ and flat roof are shown in Fig. 3. The calculation of conduction heat transfer trough the roof of solid domain is limited by the roof construction size. Algebraic grid is generated in this domain. For a typical 180° rim angle, 55 × 25 grids are generated.

In this study transient two-dimensional heat transfer simulation is made numerically based on turbulent forced convection over the roof, when the wind approaches with boundary layer profile and solar irradiation take places simultaneously over the roof. Governing equations of fluid flow and energy are solved numerically on a staggered grid system using finite volume method with SIMPLE algorithm. These governing equations are non-dimensionalized and transformed into curvilinear coordinate. The conservation equations are integrated over a control volume, and then Gauss theorem is used to transform the volume integrals into surface integrals. The power law scheme is employed for discretizing convection terms in the fluid flow and energy equations. Conduction equation is discretized by the Crank-Nicolson method [18], which has advantages for the convergence condition for using large time steps.

Initial temperature condition is one of the most effective parameter which should be considered for possible rapid convergence. In order to impose an appropriate initial temperature distribution, the computer program is run for 24 h of daytime and the resulted temperature distribution is considered for the initial condition. Energy and conduction Eqs. (10) and (11) are coupled by the roof surface condition Eq. (18) and solved simultaneously by implicit method. Corresponding time step is considered as 7 s. However temperature variation of roof and ambient air in this short time step is negligible, but accuracy of calculation especially temperature distribution through roof layer increases by using small time steps. Converged solution during a day is obtained by repeating calculation for two consecutive days with the same ambient temperature variation and constant wind velocity profile and direction. Convergence is achieved when the summation of all residuals

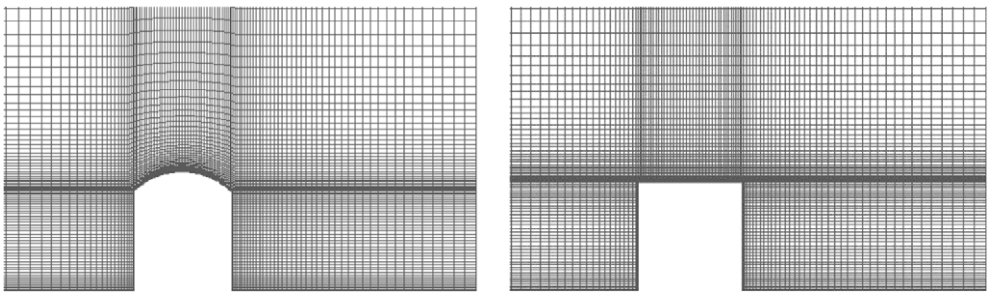

Fig. 3. Grid configuration for a vaulted roof building of $\theta_0 = 90°$ and flat roof.

for energy equation is less than 10^6 and for momentum equation is less than 10^5. Under relaxation factor is used for all velocity components, pressure, turbulent variables and temperature.

Convection heat transfer on the external surface is calculated by the following relations:

$$q'' = \frac{(T_{ex} - T_p)\rho C_P C_\mu^{1/4} k_p^{1/2}}{T_p^+} \tag{19}$$

$$\text{where,} \quad T_p^+ = Pr_t \left[\frac{1}{\kappa} \ln(Ey^+) + P \right] \tag{20}$$

$$y^+ = \frac{(C_D C_\mu)^{0.25} k_p^{0.5} y_p}{v} \tag{21}$$

The empirical P function of Jayetilleke [20] is given by:

$$P = 9.24 \left[\left(\frac{Pr}{Pr_t} \right)^{3/4} - 1 \right] \left[1 + 0.28 \exp\left(-0.007 \frac{Pr}{Pr_t} \right) \right] \tag{22}$$

T_p is the temperature of the first point near the wall. Convection heat transfer coefficient is obtained by $h = q''/(T_{ex} - T_a)$, where T_{ex} is external roof surface temperature. Based on the convection coefficient calculated above, Nusselt number is determined from the following relation:

$$Nu = hH/\lambda_a \tag{23}$$

where H is the height (which is equal to width) of the building and λ_a the thermal conductivity of the ambient air.

4.2. Model validation

Simple flow problem such as fully developed turbulent flow in a duct and turbulent flow over a backward step for which the solutions are available, compared with the developed numerical code. The result of fully developed flow in duct found good agreement with Kakas [21] correlation as described in [13]. Turbulent flow over a backward facing step is widely used to evaluate the performance of turbulence models in the prediction of separated flows. For the numerical validation, the flow configuration of Kim et al. [22] has been selected. In this case for the domain sketched in Fig. 4, the ratio of step height to outlet channel height is taken 1:3 and Reynolds number is 46,000. Reattachment length based on the developed code of this study is obtained as 6.94H while for Kim et al. [22] is 6.5H–7.5H. Streamlines for flow over the backward facing step and reliable span of X_r are presented in Fig. 5. It shows that the developed RNG k–ε code has good agreement with other studies.

5. Results and discussion

For a two-dimensional turbulent flow, simulation is made to find air flow and heat transfer from a building with various roofs. Variation of Nusselt number for various conditions and also heat flow to the buildings are determined for different types of roofs. Wind flow profiles are assumed to blow in four directions which are

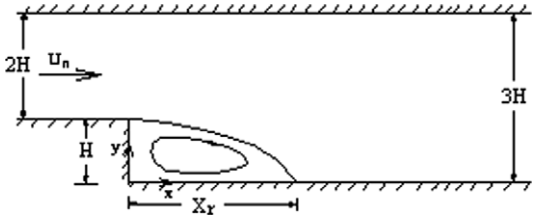

Fig. 4. Geometry of the backward facing step flow.

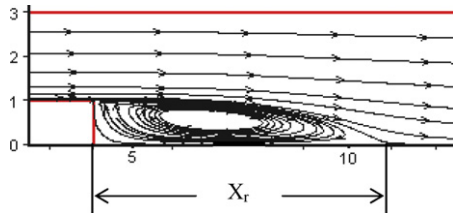

Fig. 5. Path lines for flow over the backward facing step.

shown in Fig. 2. For buildings with north-south orientation, it is assumed that wind flows either from east or from west. For a building arrangement along east-west, wind is taken to blow from north or from south. Such building orientations are the preferred construction direction due to both religious consideration and passive cooling effect in summer period.

Numerical calculations are made for climatic condition of Yazd (31.9°N) at the first day of September. This city is famous for its high-rise wind catchers (Baudgir). The province of Yazd situated in the central part of the country with typical hot and dry desert summer condition. T_{max} and T_{min} of this city in the first day of September are 34 °C and 17 °C, respectively [13,14]. Variation of ambient air temperature and horizontal irradiation along the day for Yazd at the first day of September are shown in Fig. 6. Dominant wind during summer period blows from west or north west with averaged maximum speed of 4.4 m/s [23]. Other parameters used for calculations are listed in Table 3.

Numerical simulation is made for different rim angles of 90°, 120°, 150°, and 180° of vaulted roofs. Various Reynolds number of 5×10^5, 10^6, 2×10^6 of wind flow are considered which corresponds to velocities of U_∞ equal to 2.5, 5, 10 m/s. Most of these speeds are in the range of wind velocity which may occurs during summer period in Yazd. To determine the amount of heat flux passes from roof into the interior of an air-conditioned space, the thickness of the roof is taken as a single layer $t = 30$ cm and the temperature of inner layer of the roof is considered constant 27 °C. For an air-conditioning building with interior temperature of 25 °C, the assumption of 27 °C for the ceiling surface due to stratification is acceptable. Height of vertical walls are assumed 4 m which is normally in the range of the traditional construction and the width of all building cases are taken 4 m. The buildings length normal to the page are assumed large in order to consider two dimensional

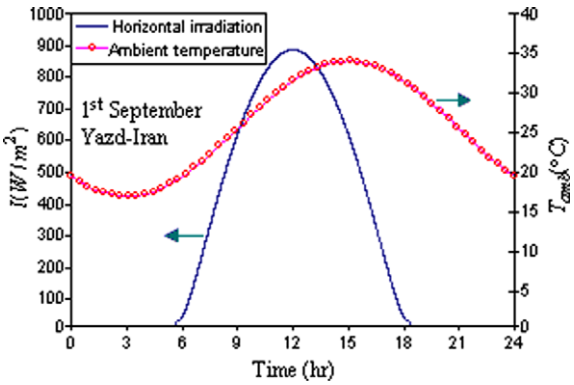

Fig. 6. Time variation of horizontal irradiation and ambient temperature used for the numerical calculation.

Table 3
Parameters used for simulation

Roof: single layer (mud brick)	Thickness = 0.3 m, $\rho C_p = 857$ kJ/m^3 K, $\lambda = 0.6$ W/m K
Outdoor air	$\rho C_p = 1200$ J/m^3 K, $\upsilon = 2 \times 10^{-5}$ m^2/s, $\lambda = 0.028$ W/m K
Others	$\sigma = 5.67 \times 10^{-8}$ W/m^2 K^4, $\varepsilon = 0.8$, $\alpha = 0.7$, $\rho_g = 0.2$, $T_{in} = 27$°C CF = 0.155

condition and neglect the end effects on flow field around the roof and heat transfer through the roof. Such assumption may not be valid for roofs with short length of vary tall buildings. Natural convection over the roof found negligible for similar studies [13]. Ground surface and the vertical walls are assumed insulated. Flow field around various building is investigated and corresponding studies are made to find temperature distribution of the external roof surface temperature and heat flow to the building.

For the rest of this article, east-wind, west-wind, north-wind and south-wind directions are referred to case A, case B, case C and case D respectively which their schematics are presented in Fig. 2. East-wind and west-wind were considered to blow to an east-west faced vaulted roof building and for a north-south faced vaulted roof building, wind will blow from north or south. For a north-south building, x-direction component of roof is imposed from the east side of the building as shown in Fig. 1 and for an east-west faced building, x-direction component of roof is taken from the north position.

5.1. Flow field around buildings

Flow patterns around flat and vaulted roof buildings consists of some eddies and recirculation regions. For flat roof separation start at leading edge while for vaulted roof separation occurs after the roof top. Path lines for vaulted roof with rim angle of 150° and flat roof at $Re = 5 \times 10^5$ are presented in Fig. 7. Reattachment length increases slightly by increasing flow Reynolds number but its variation with rim angle of the vaulted roofs is more significant [7,13,14].

Pressure contours for vaulted roof with 150° rim angle and flat roof at $Re = 5 \times 10^5$ are illustrated in Fig. 8. Pressure is high in the front side of the building, because of flow stagnation and vacuum pressure maintained on the leeward wall due to flow recirculation. Pressure variation is considerable over the roof, while in the front and back side of the buildings, pressures are nearly uniform. Higher air velocities and strong pressure difference for vaulted roofs is observable by comparing the result of contours of velocity and pressure for the vaulted and flat roofs [7,13,14].

Due to higher pressure differences for vaulted roof, ventilation rate would be higher when apertures are open in forward wall and roof top. This is usually imposes during the night time, when out-door air temperature is low and ventilation cools the building for summer conditions in hot arid regions [5].

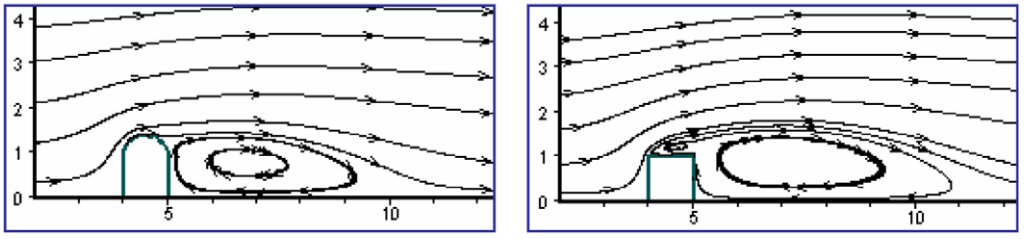

Fig. 7. Path lines for 150° rim angle of vaulted and flat roofs at $Re = 5 \times 10^5$.

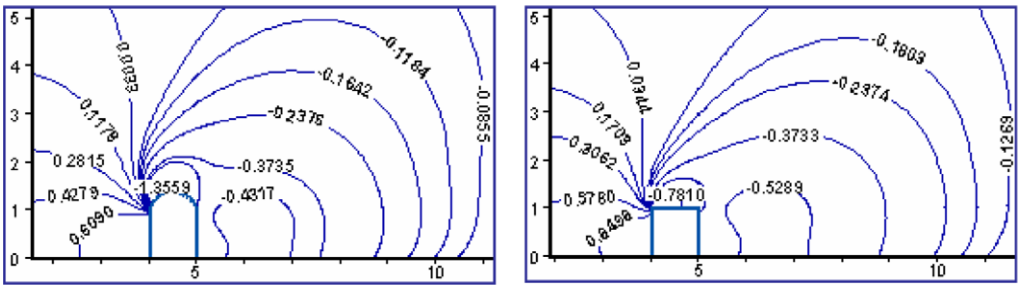

Fig. 8. Pressure contours over vaulted roof for 150° rim and flat roof at $Re = 5 \times 10^5$.

5.2. Heat transfer

One particular characteristic of the dome-type roof is the auto-shading effect, which occurs most of the day except at noon. On the other hands, solar intensity on a dome is not uniform over its entire surface. Depending on the hour of the day, a portion of the surface receives strong direct sunbeams, while the other parts of the curved surface stay in shade [1,13].

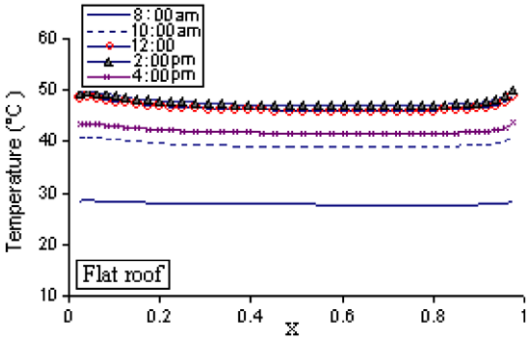

Fig. 9. Flat roof temperature distribution at various hours, $Re = 10^6$.

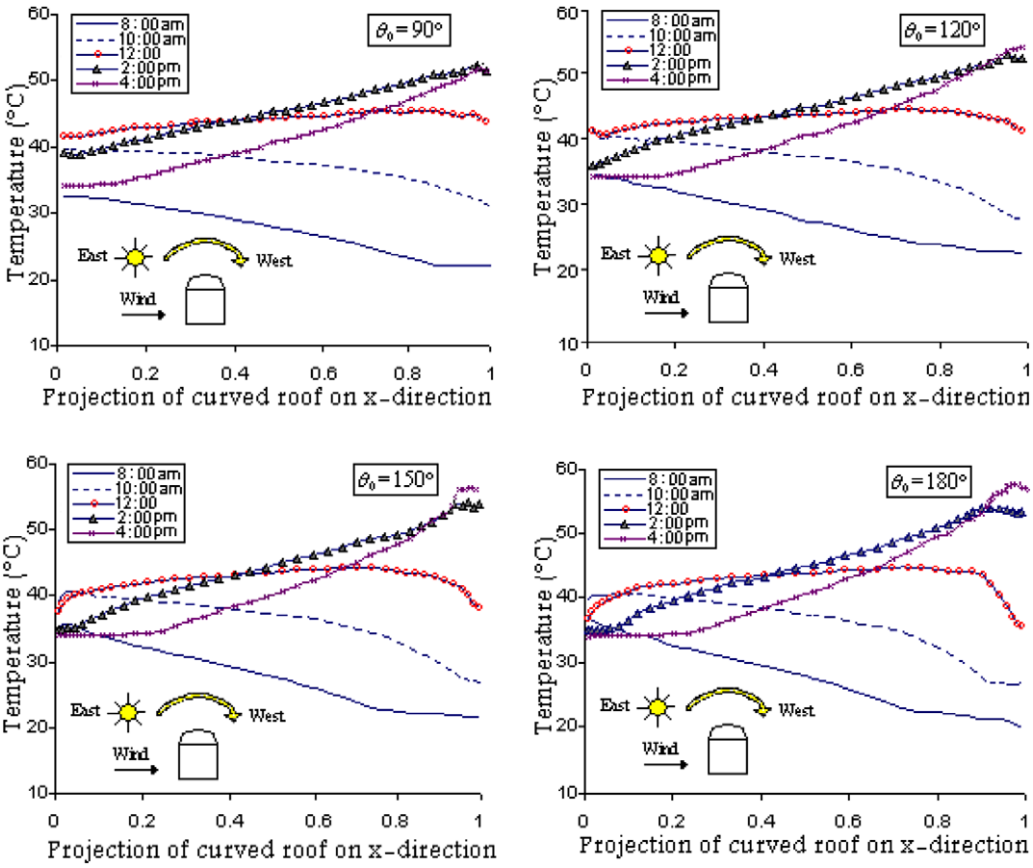

Fig. 10. North-south vault roof surface temperature distribution, Case A, east wind and $Re = 10^6$.

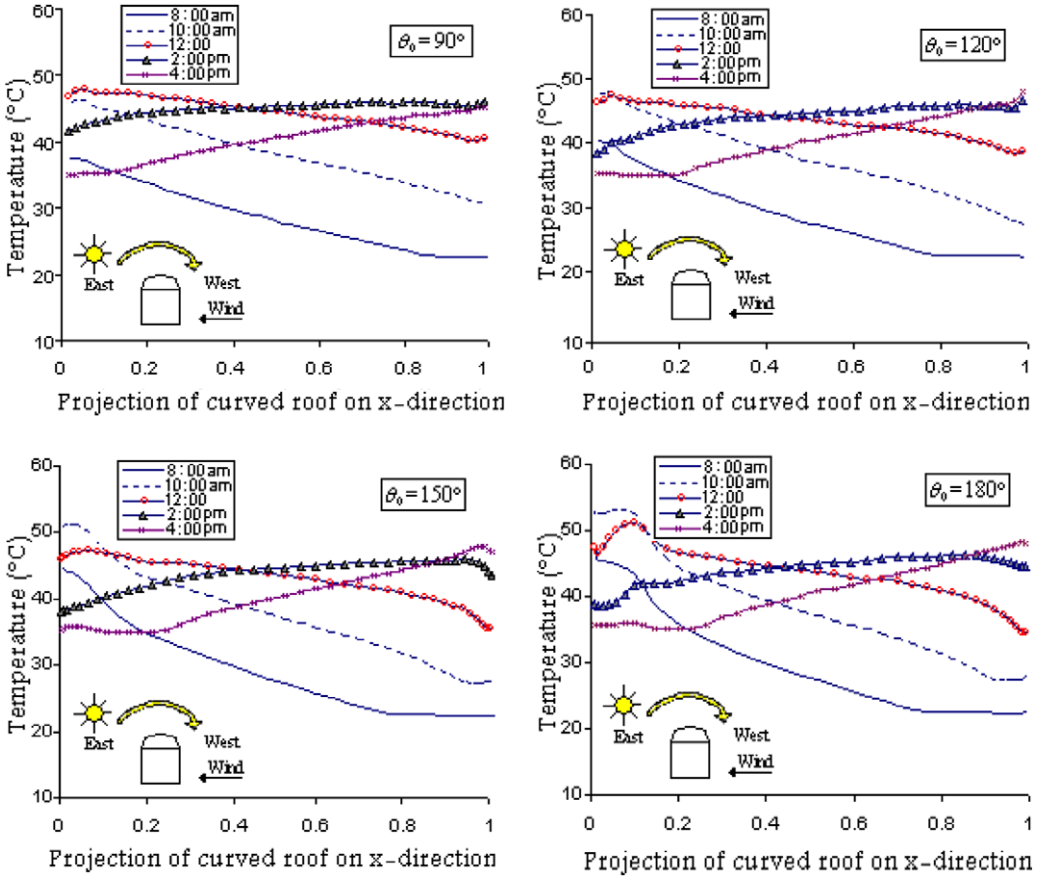

Fig. 11. North-south vaulted roof surface temperature distribution, Case B, west wind and $Re = 10^6$.

A typical roof temperature distribution for flat roof is shown in Fig. 9. Temperature distribution over vaulted roofs for rim angles of 90°, 120°, 150° and 180° and various direction of wind flow, building orientations and $Re = 10^6$ are illustrated in Figs. 10–13. Roof surface temperature distribution for flat roof is nearly uniform but it varies for vaulted roofs, depending on rim angle, wind direction and building orientation.

In the morning, the east part of a north-south orientation vaulted roof building is exposed to direct beam radiation when the west part of it is in shade but in the afternoon it happens vise versa. Temperature of eastern part of a vaulted roof for the case A is lower than case B in the morning. For east wind, case A, the eastern part of vaulted roof has higher convection coefficient comparing with western parts. West part of vaulted roofs exposes to solar direct radiation in the afternoon where convection coefficient is low for case A. Temperature of western part of vaulted roof for case A is more than case B, because of lower convection coefficient on this part. Therefore, the temperature difference between eastern and western part of vaulted roof for case A in Fig. 8 is more considerable than case B in Fig. 9. By increasing the rim angle of the vaulted roof the shading part of the vault increases, so the temperature difference between the eastern and western part of the vault increases. This difference is high in the afternoon especially for the case A.

For an east-west vaulted roof, northern part of vault is always in shade but south part of it exposes to direct solar radiation most of the time during the day. In the case of north-south wind flow, case C, the leeward section of vault, which is south part of it, has lower convection coefficient comparing with north part. So the temperature difference of case C is more than others cases as shown in Fig. 12. Temperature distribution of south part of vault for the case D, Fig. 13, is lower than case C due to higher convection coefficient in this part. Variation of temperature distributions for case D is more flat than other cases.

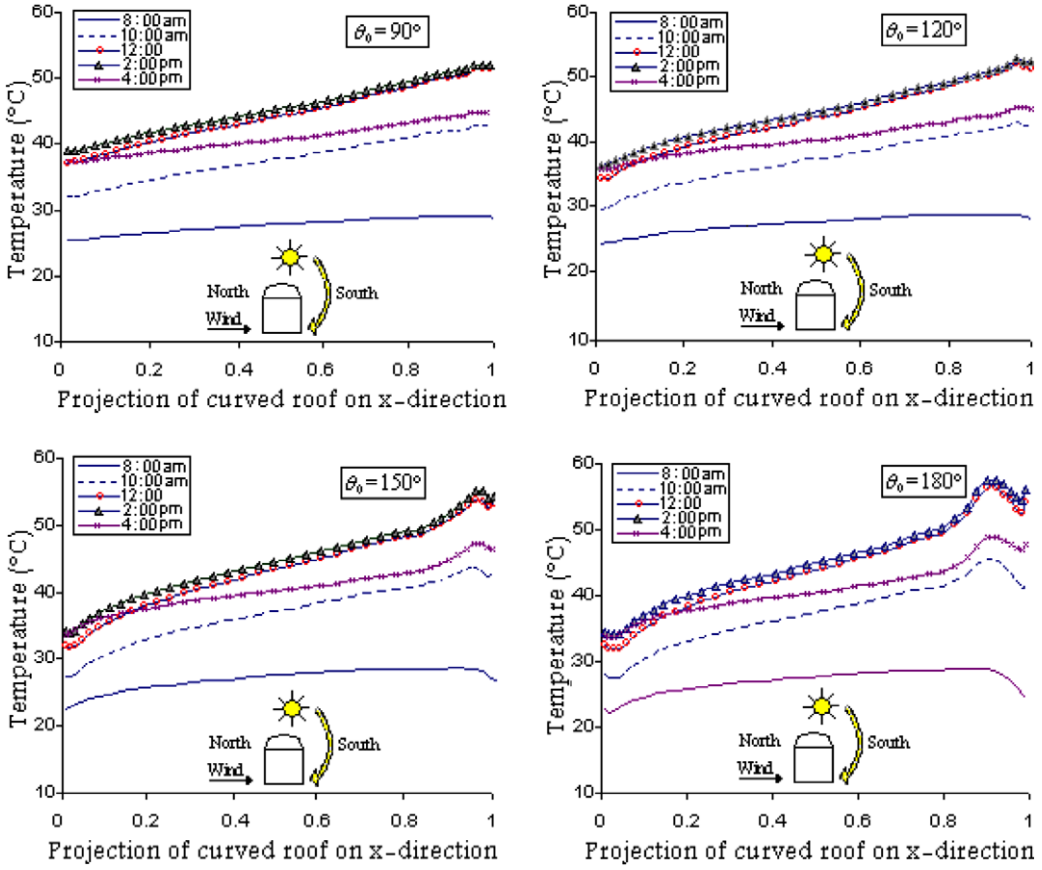

Fig. 12. East-west vault roof surface temperature distribution, Case C, north wind and $Re = 10^6$.

Flat roof surface temperature is more than the temperature of vaulted roof pick point for different rim angles, because of its lower convection heat transfer coefficient of flat roof. However, Tang et al. [11,12] reported equal temperature for top of vaulted roof and flat roof due to the assumption of the same amount of convection coefficient along the vaulted and flat roofs. Temperature distribution along the roof decreases with increasing Reynolds number because of higher convection heat transfer with ambient air.

Convection coefficient along the vaulted roofs varies due to variation of flow over the curved roofs. Local Nusselt number is calculated for flat roof and different vault based on Eq. (23). Nusselt number variation at $Re = 5 \times 10^5$ for the cases A, B, C and D are illustrated in Fig. 14. According to the definition of x-direction for roofs shown in Fig. 1, for the cases A and C the leeward side of vaulted roof has lower Nusselt number than forward side, because of the effects of air flow separation on the back side but for cases B and D it is vise versa. Separation of flow causes the forced convection coefficient to decrease. For lower rim angles, separation tack places farther away near the end of roof, so for those vaulted roofs average Nusselt number is more than higher rim angles of vaulted roofs. It should be noted that Nusselt numbers are constant during the day for the range of Reynolds number studied by assuming that air physical properties have no significant variation and independent of solar radiation.

The rate of heat transfer from the roof to the room is determined by taking integral of heat flow over the entire grids. The averaged heat transfer rate is determined for various roof rim angles of vaulted roof as well as for flat roof. For an east-west orientation building with south wind, case D, heat flow decreases considerably as compared with other cases. For the case D, rim angles lower than 150° has lower heat flow comparing with flat roof, however, heat flow of 180° rim angle is a little more than flat roof.

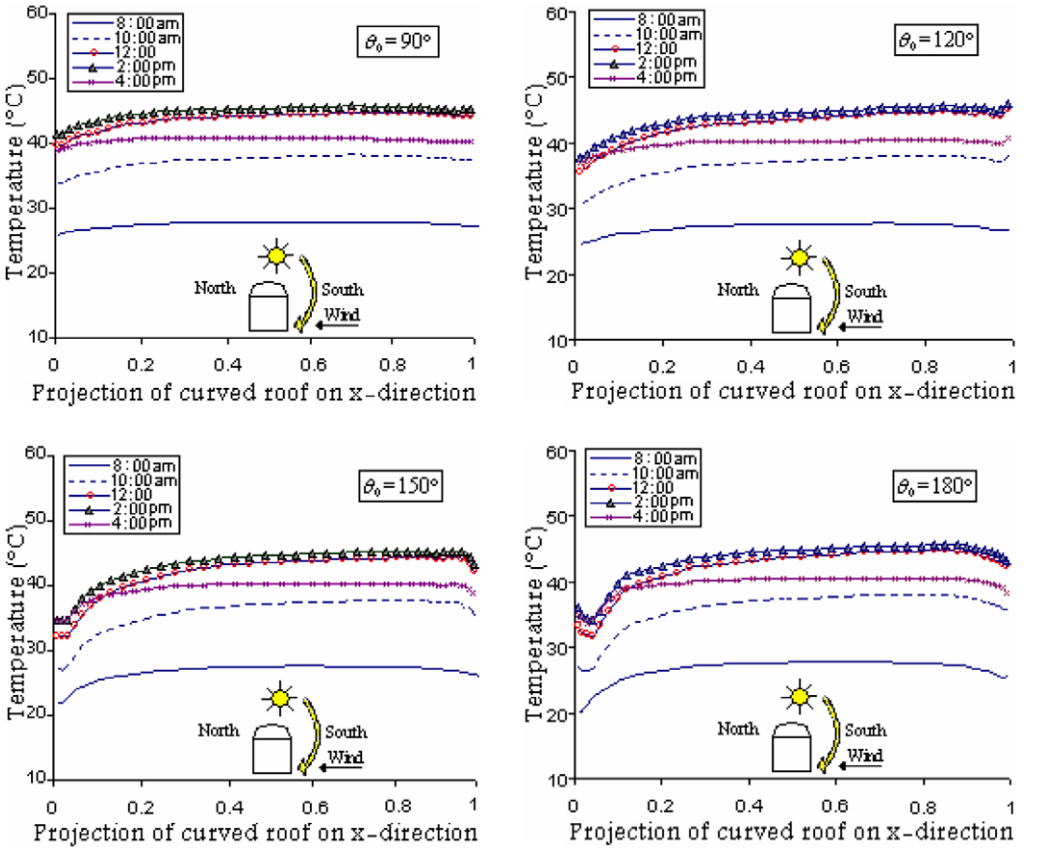

Fig. 13. East-west vault roof surface temperature distribution, Case D, south wind and $Re = 10^6$.

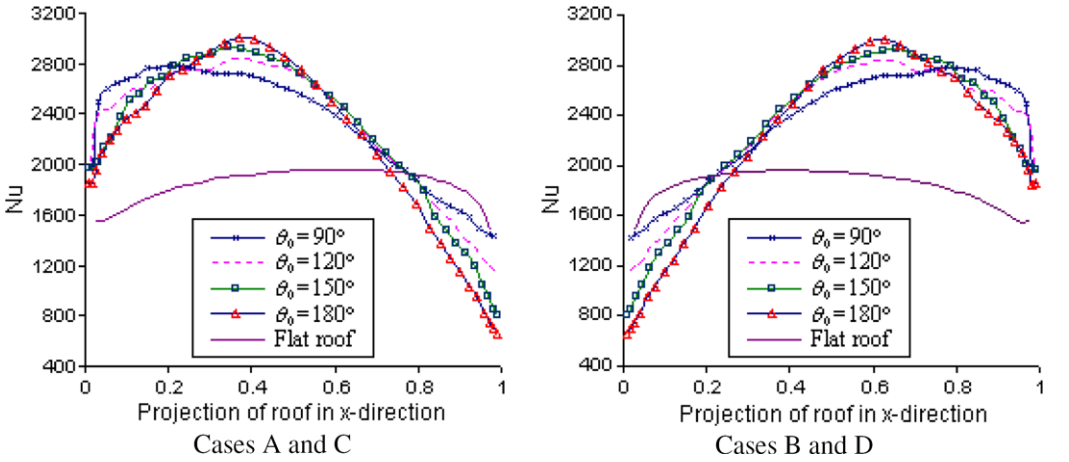

Fig. 14. Nusselt number distribution for various roofs at $Re = 5 \times 10^5$.

Average daily heat flux to different roofs for cases A, B, C and D of wind flow is presented in Table 4. According to the results of this table, the amount of daily heat flow per unit area for a north-south vaulted roof, cases A and B, is lower than flat roof except for rim angle of 180° which is slightly more than flat roof. But for cases C and D averaged heat flow to the room decreases remarkably by increasing the rim angle of

Table 4
Daily average heat flow through different roofs (W h/m^2)

Case	*Re*	θ_0				
		90°	120°	150°	180°	Flat
A	5×10^5	884.5	885.7	954.3	1102.5	1093.8
B	5×10^5	875.2	878.4	969.3	1121.2	1093.8
C	5×10^5	850.5	782.4	754.1	704	1093.8
D	5×10^5	799.1	651.6	378.2	286.1	1093.8
A	10^6	496.1	498.4	539.8	607.5	599.2
B	10^6	487.9	490.5	545.1	618.3	599.2
C	10^6	469.3	436.8	421.4	376.6	599.2
D	10^6	427.5	342.1	191.5	142.7	599.2

Case A: East-wind flow direction, Case B: west-wind flow direction.
Case C: North-wind flow direction, Case D: south-wind flow direction.

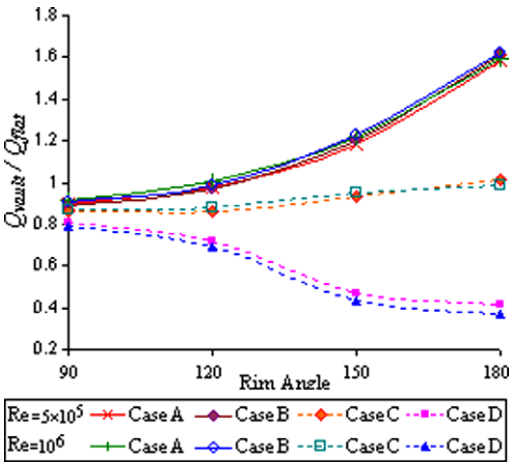

Fig. 15. The ratio of Q_{vault}/Q_{flat} for various rim angles and Reynolds numbers.

vaulted roof. Daily heat flow, Q is determined for each case and the ratio of Q_{vault}/Q_{flat} for various rim angles and Reynolds numbers is presented in Fig. 15. For rim angles less than 120° this ratio is lower than flat roof for all cases. Q_{vault}/Q_{flat} increases by rim angles of vaulted roof for all cases except case D which in this case reduction of this ratio is remarkable.

Buildings with vaulted roofs have much favorable thermal condition in comparison to flat roofs during the night and early morning which can be one of the reasons of using these kinds of roofs in hot arid regions [13].

6. Conclusion

From the analysis of heat transfer and fluid flow over vaulted roof and flat roof buildings, the following conclusions are obtained:

1. Convection coefficient over vaulted roof is significantly higher, on the forward side and decreases after separation on the leeward side, but its variation for flat roof is not considerable.
2. Temperature varies along the vaulted roofs during the day as a result of the auto shading of roofs but for flat roofs temperature distribution along the roof is nearly uniform. Temperature difference of two sides of vaulted roofs increases with rim angle.
3. For a vaulted roof building along north-south, case A, when wind blows from east and also for a vaulted roof building along east-west when exposed to north wind, Case C, temperature difference between the two sides of vault is more than two other cases.

4. Daily heat flow for case D, (north-south faced of vaulted roof when wind blows from south) is significantly lower than other cases and flat roof. This orientation will have also winter advantages for high solar exposure from south.
5. For all rim angles of vaulted roof and various wind flow direction, heat flow is lower than flat roof during the night and early in the morning.

References

[1] Sabzevari A, Golneshan AA. Solar radiation intensity on domed roofs. Solar Wind Technol 1990;7(6):625–47.
[2] Bahadori MN, Haghighat F. Performance of adobe structures with domed roofs and moist internal surfaces. Thermal Solar Energ 1986;36(4):365–75.
[3] Mainstone RJ. Developments in structural form. Cambridge: MIT Press; 1983, p. 95–136.
[4] Fathy H. Natural energy and vernacular architecture. Chicago, London: University of Chicago Press; 1986.
[5] Yaghoubi M. Air flow patterns around domed roof buildings. Renewable Energ 1991;314(1):45–350.
[6] Sabzevari A, Yaghoubi M. Air flow behavior in and around domed roof buildings. Wind Eng 1992;16(1):27–34.
[7] Hadavand M, Yaghoubi M, Emdad H. 2D analysis of turbulence wind flow around vaulted roofs and flat roofs. In: Proceedings of the 10th fluid dynamics conference, Yazd, Iran; 2006.
[8] Pearlmutter D. Roof geometry as a determinant of thermal behavior: a comparative study of vaulted and flat surface in a hot-arid zone. Architect Sci Rev 1993;36(2):75–86.
[9] Gadi MB. Design and simulation of a new energy conscious system (basic concept). Appl Energ 2000;65(1–4):349–53.
[10] Tang R, Meir IA, Etzion Y. An analysis of absorbed radiation by domed and vaulted roofs as compared with flat roofs. Energ Building 2003;35(6):539–48.
[11] Tang R, Meir IA, Etzion Y. Thermal behavior of building with curved roofs as compared with flat roofs. Solar Energ 2003;74(4):273–86.
[12] Tang R, Meir IA, Tong WU. Thermal performance of non air-conditioned buildings with vaulted roofs in comparison with flat roofs. Building Environ 2006;41(3):268–76.
[13] Hadavand M, Yaghoubi M, Emdad H. Thermal analysis of vaulted roofs. Energ Building 2008;40:265–75.
[14] Hadavand M, Yaghoubi M, Emdad H. Thermal exchange of flat and vaulted roofs exposed to solar radiation for various building geometries. In: Proceedings of the 15th ISME conference, Tehran, Iran; 2007.
[15] Yakhot V, Orszag SA, Thangman S, Gatski TB, Speziale CG. Development of turbulence models for shear flows by a double expansion technique. Phys. Fluid 1992;4(7):1510–20.
[16] Duffie JA, Beckman WA. Solar energy engineering of thermal processes. 2nd ed. A Wiley-Interscience Publication; 1991.
[17] Daneshyar M. Solar radiation statistics for Iran. Solar Energ 1978;21(4):345–9.
[18] Anderson DA, Tannehill JC, Pletcher RH. Computational fluid dynamics and heat transfer. New York: McGraw-Hill; 1984.
[19] Launder BE, Spalding DB. The numerical computation of turbulent flows. Comput Meth Appl Mech Eng 1974;3(2):269–89.
[20] Jayatilleke CLV. The influence of Prandtl number and surface roughness on the resistance of laminar sub-layer to momentum and heat transfer. Prog Heat Mass Transf 1969;1:193–329.
[21] Kakas S, Shah RK, Aung W. Handbook of single-phase convective heat transfer. John Wiley and Sons; 1987.
[22] Kim J, Kline SJ, Johnston JP. Investigation of a reattaching turbulent shear layer: flow over a backward-facing step. Fluid Eng 1980;102:302–8.
[23] Kasmai M. Climate architecture. 2nd ed. Khak Publication; 2003 [in Persian].